J. Phys. B: At. Mol. Opt. Phys. **21** (1988) 2129-2144. Printed in the UK

Ionisation of Ti^+, Ti^{2+} and Ar^{2+} by electron impact

M J Diserens†§, A C H Smith† and M F A Harrison‡

† Department of Physics and Astronomy, University College London, London WC1E 6BT, UK

‡ Culham Laboratory (Euratom/UKAEA Fusion Association), Abingdon, Oxon OX14 3DB, UK

Received 24 February 1988

Abstract. Cross sections for the single ionisation of Ti^+, Ti^{2+} and Ar^{2+} by electron impact have been measured in the energy range from the thresholds to 2000, 2000 and 1250 eV respectively using the fast crossed beams technique. The cross sections for Ti^{2+} and Ar^{2+} are compared with previously measured cross sections and with those given by the semi-empirical formula of Burgess and Chidichimo. The cross section for Ti^+ has not been measured previously and is compared with those given by the Lotz formula and the McGuire scaled plane-wave Born approximation.

1. Introduction

In fusion plasma devices complex atoms are driven, sputtered or may be injected from the walls of the containment vessel and become progressively more ionised and excited in collisions with electrons as they penetrate into the plasma. The resulting radiation from the excited atoms and ions can represent a significant energy loss from the plasma and may alter the temperature profile. In the analysis of plasmas containing impurities, the cross sections for electron impact ionisation of the impurity elements in various stages of ionisation are needed. The current programme of research at Culham Laboratory includes experiments to measure the ionisation cross sections of low-charge ions and atoms of elements likely to occur as impurities in fusion plasmas.

The present paper describes measurements of cross sections for the processes

$$e + Ti^+ \rightarrow 2e + Ti^{2+}$$

$$e + Ti^{2+} \rightarrow 2e + Ti^{3+}$$

$$e + Ar^{2+} \rightarrow 2e + Ar^{3+}.$$

Titanium is a metal commonly encountered in fusion plasma devices and argon is a gas that may be injected for diagnostic purposes.

The ionisation cross section of Ti^+ has not been measured previously, but a measurement for Ti^{2+} has been reported by Mueller *et al* (1985). Their cross section exhibits considerable structure and it is important to examine whether this is a consequence of the type of ion source that was used. In their source metal ions are

§ Present address: Amersham International plc, Amersham, Bucks HP7 0HJ, UK.

0953-4075/88/112129+16$02.50

produced by an unknown sequence of electron impact dissociation and ionisation of metal chlorides and so the ion beam may contain a high population of metastable excited ions. In our source the ions are produced by straightforward electron impact ionisation of sputtered atoms. The presence of metastable excited ions in the beam is possibly less likely or at least the metastable fraction will be different.

Ionisation of Ar^{2+} has been investigated by two groups comparatively recently (Danjo *et al* 1984, Mueller *et al* 1985). The present measurement provides a particularly good check for systematic errors by comparing an absolute value of a cross section measured in this laboratory with those of the other two laboratories because relatively intense beams of Ar^{2+} are obtainable and accurate cross sections are thus more easily measured.

The data presented in this paper were initially reported at the 14th International Conference on the Physics of Electronic and Atomic Collisions (Diserens *et al* 1985).

2. Experimental method

2.1. The apparatus

The fast crossed electron–ion beams technique has been employed in the present experiments. The technique and the performance of the Culham apparatus have been described by Montague *et al* (1984) in their paper on ionisation of helium atoms. For the present work the apparatus was fitted with a sputter ion source developed from a design of Hill and Nelson (1965). Details are given by Man *et al* (1987a). When Ti^+ or Ti^{2+} ions are required, a potential of -1 kV is applied to the titanium sputter electrode. Argon ions from the support gas bombard the electrode; titanium atoms are sputtered into the plasma, become ionised and are extracted to form the ion beam. Alternatively, when Ar^{2+} ions are required, no potential is applied to the sputter electrode and argon ions are extracted directly from the source.

For the present studies, a new type of focusing electron gun, developed specifically for use with metal atoms and ions, was used for the first time. Some of the data for Ti^+ were obtained using the earlier planar-grid gun. The new gun has been used subsequently for measurements on other metal ions (Man *et al* 1987a, b, c). The gun produces a ribbon beam 1.6 mm × 25 mm in section with a usable current and energy of 7 μA at 5 eV to 1000 μA at 2000 eV. The two-stage gun is shown schematically in figure 1(*a*). In the first stage a large accelerating potential is used to overcome the space charge in front of the cathode. In the second stage the electrons are retarded or accelerated to the required final energy and are focused on to the ion beam target. The first stage (Klemperer 1947) is similar to the immersion objective of Soa (1959), but with rectangular instead of circular apertures. It consists of a strip cathode followed by a control electrode and an accelerating electrode, both having slit apertures. The cathode is an impregnated tungsten dispenser cathode (Semicon M-type, Walmore Electronics Ltd), which has an emissive area of 2 mm × 25 mm. This type of cathode is readily reactivated after exposure to air. The first stage generates a virtual object a small distance behind the cathode.

The second stage of the gun consists of a three-element rectangular tube lens designed using the data of Harting and Read (1976). The first element is at the same potential as the accelerating electrode and the third element is at the same potential

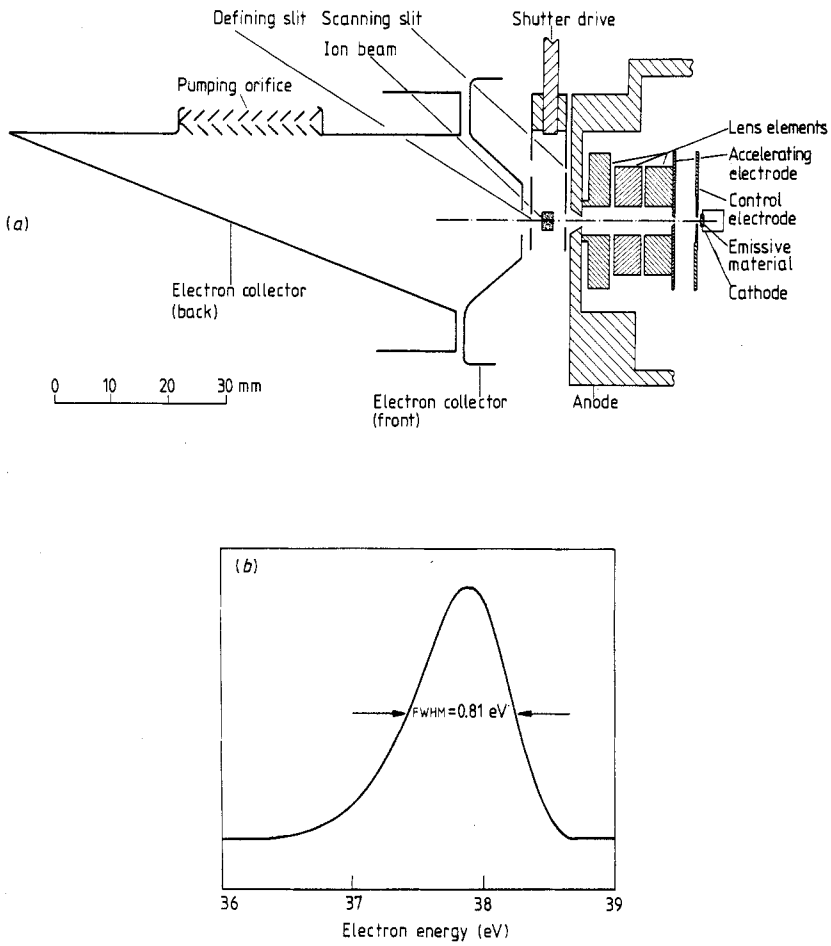

Figure 1. (*a*) Section through the new electron gun, collision region and electron collector. (*b*) Energy distribution of the electron beam produced with the new gun. The cathode-to-anode potential difference was 39.5 V and the beam current was 800 μA.

as the anode (normally at earth potential). The upper and lower parts of the second element are isolated from each other so that a small potential can be applied between them to steer the electron beam through the anode aperture. This feature is particularly useful at low energies. By adjustment of the mean potential of the second element, the electron beam is focused through the anode aperture and an image of the virtual object is produced between the collision region and infinity.

The performance of the new gun is better than the previous gun in several respects. Firstly, a useful electron beam current is available to lower energies, thus allowing cross section measurements to be made down to the usually low thresholds for ionisation of metal atoms and ions. Secondly, higher electron energies can be attained so that our cross section measurements are now normally extended to 2000 eV. Previously the energy was usually limited to 750 eV because of arcing between the closely spaced

grid electrodes or across interelectrode insulators. Thirdly, the electron energy distribution is narrower and more symmetrical so that the measured shape of a cross section near threshold is more certain and structures in cross sections are better resolved. The value of this improvement is particularly apparent in the measurements on Ti^{2+} reported in this paper. A typical electron energy distribution is shown in figure 1(*b*). The FWHM of the distribution depends on the electron current and varies from 0.5 eV at 250 μA to 0.9 eV at 1000 μA. Currents in the experiments described in this paper were usually not more than 250 μA.

2.2. Procedure

As in previous work the cross section measurements for each ion species were made at two target ion energies to test for spurious effects. The product ion detector (Johnstone Laboratories electron multiplier type MM1) was calibrated at each energy by directing a beam of ions from the ion source alternatively into the detector or into a Faraday cup connected to an electrometer. The calibration beam species and energy ideally corresponded to those of the product species in the experiment, but this was not always possible (see §§ 3.2.1 and 3.3).

The detection efficiency tended to be variable for all three ions and therefore frequent calibrations were performed. The error in this measurement was the largest component of the total error of the measured cross sections. Typical ion beam and detector characteristics for the three sets of measurements are shown in table 1.

Table 1. Typical ion beam and detector characteristics.

Target ion	Ion beam energy (keV)	Typical current (A)	Typical product ion detection efficiency	Typical signal-to-background ratio
Ti^+	2	5×10^{-10}	0.535 ± 0.009	30:1
	4	2×10^{-9}	0.789 ± 0.011	6:1
Ti^{2+}	4	3×10^{-11}	0.789 ± 0.032†	4:1
	6	4×10^{-11}	0.937 ± 0.037†	4:1
Ar^{2+}	3.33	1×10^{-9}	0.797 ± 0.012†‡	17:1

† Measured indirectly (see §§ 3.2.1 and 3.3).
‡ Same velocity as Ti^{2+} at 4 keV.

For each ion species, linearity of the signal with electron current was demonstrated at several electron energies. The cross sections determined from these data have smaller random errors and are identified in figures 4, 5 and 6 for Ti^{2+} and Ar^{2+}, but not in figure 2 for Ti^+ because in this case the random errors of all points are negligible.

In order to obtain a better representation of structures and other rapidly varying parts of the cross section curves, some data were obtained by stepping through a small energy range in a short time compared with the time in which a significant drift in the ion detection efficiency occurred. The scan was repeated several times to reduce the statistical errors. These data are later referred to as 'energy scan data'.

The contact potential of the electron gun (i.e. the correction applied to the negative cathode potential to obtain the true mean electron energy in eV) was determined from

observations of the threshold for ionisation of Ne^+ to Ne^{2+}. For the old gun used in obtaining some of the Ti^+ data, the contact potential was somewhat variable but averaged 2.0 ± 0.5 V. For the new focusing gun the value was consistently 1.7 ± 0.5 V.

The effective height h' of the ion beam was determined frequently using a computer-controlled scanning slit (Montague *et al* 1984). The computer calculated h' from the overlap integral of the vertical intensity profiles of the two beams. The ion beam was always adjusted to make its profile nearly uniform so that h' was close to the geometrical height of the ion beam (2.5 mm). This minimised any errors inherent in the scanning shutter technique (Montague *et al* 1984).

3. Results and discussion

3.1. Ti^+

3.1.1. Results. Measurements were made with Ti^+ beam energies of 2 and 4 keV. The shapes of the cross section curves obtained at the two energies were in good agreement, but the absolute values of the 2 keV data tended to be a few per cent smaller (4–11%) and more variable. This was attributed to variations and errors in the efficiency ε of the product ion detector. The lower value of ε for 2 keV was more susceptible to variations in the surface condition of the first dynode of the electron multiplier. The values of ε at 4 keV over a period of several months were much more consistent and the cross sections determined using these calibrations were in good agreement. However, the difference between the mean values of the cross sections taken at the two ion energies are within the 90% confidence limits of the two sets and consequently the data taken at 2 keV have been normalised to the data at 4 keV.

The data are shown in figure 2. The full curve below 40 eV is the average taken over the energy scan data, and above this energy it is a best-fit line to the data points. Values of the measured cross section represented by this line are listed in table 2 together with total errors. Above 40 eV the random error has been calculated from the deviations of the experimental points from the smooth curve and below 40 eV from scatter in the scan data. Systematic errors arise from the uncertainty in the multiplier efficiency (±3%), the effective beam height measurement (±1.5%) and the beam current measurements (±2%). These have been compounded in quadrature with the random errors to give the total errors. In figure 2 the points shown below 40 eV are for comparison with the scan data and demonstrate the scatter due to slight variations in the contact potential. Ninety per cent confidence limits on the counting statistics are less than 1% of the peak cross section and are smaller than the size of the symbols. Confidence limits on the scan data are of the same order.

Also shown in figure 2 are curves calculated from the semi-empirical formula of Lotz (1969) and the scaled plane-wave Born approximation of McGuire (1977). The values for inner-shell binding energy for the Lotz formula are taken from Lotz (1968) and allow for the possibility of ionisation of the 3d electrons. The Lotz value for the binding energy of the 3p electrons is used in the McGuire formula, but the binding energy of 3d electrons is taken from Corliss and Sugar (1979).

3.1.2. Discussion. The measured cross section of Ti^+ shows a main threshold lying between 13.0 and 13.5 eV, with a lower threshold lying at 12.0 eV. A large increase in

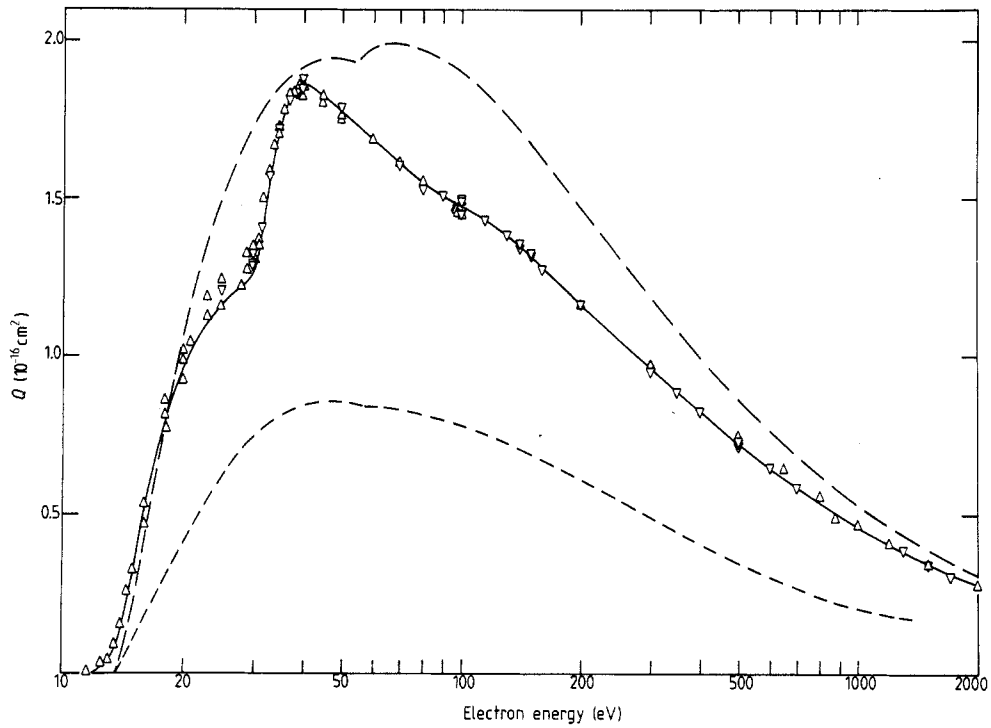

Figure 2. Electron impact ionisation cross section Q of Ti^+. Present results: △, ion energy 2 keV; ▽, ion energy 4 keV; ——, scans (below 40 eV) or best-fit curve through experimental points (above 40 eV); — —, formula of Lotz (1969); - - -, scaled plane-wave Born approximation of McGuire (1977).

the cross section occurs from a threshold at 30 eV, apparently caused by an excitation-autoionisation process. In order to interpret these structures it is necessary to consider the processes of formation and the states of the target and product ions. Some of the relevant states are shown on the simplified energy level diagram of figure 3.

The Ti^+ ions are produced in the ion source by electron bombardment of predominantly ground-state Ti atoms. The ground state of Ti is $3p^63d^24s^2\ ^3F$. Ti^+ can be produced in the ground state $3p^63d^24s\ ^4F$ and the low-lying metastable state $3p^63d^24s\ ^2F$ by direct removal of an electron from the ground-state atom. Ions of Ti^+ may also be produced in other $3d^24s$, $3d^3$ and $3d4s^2$ configurations, but these are less likely. The thresholds for ionisation of the lowest ^4F and ^2F states are 13.6 and 13.1 eV respectively. Ionisation from these states is responsible for the main observed threshold. It is not possible to assign a particular state responsible for the threshold at 12 eV, but it could be due to the presence of ions in these numerous other states.

The strong increase of cross section from 30 eV is likely to be caused by excitation of an inner-shell electron followed by autoionisation. The lowest-energy inner-shell excited state of Ti^+ is the $3d4s4p\ ^4D$ state, but this only lies 6.48 eV above the ground state (Corliss and Sugar 1979) and cannot autoionise. Excitation of a 3d electron to higher states may contribute to the cross section through autoionisation, but the contribution would be small and would not show a distinct threshold. However, the threshold for excitation of a 3p electron lies above the ionisation threshold, so the

Table 2. Measured cross section for electron impact ionisation of Ti^+ taken from a smooth curve drawn through the experimental points of figure 2.

Mean electron energy† (eV)	Measured cross section Q (10^{-16} cm^2)	Total error in Q‡ (±% of Q)	Mean electron energy† (eV)	Measured cross section Q (10^{-16} cm^2)	Total error in Q‡ (±% of Q)
11.5	0.000		40	1.856	5
12	0.003	100	45	1.817	5
12.5	0.020	50	50	1.768	5
13	0.034	30	55	1.723	5
13.5	0.079	14	60	1.681	5
14	0.145	8	70	1.607	5
14.5	0.229	7	80	1.547	5
15	0.339	6	90	1.496	5
16	0.531	5	100	1.460	5
17	0.674	5	110	1.424	5
18	0.790	5	120	1.412	5
19	0.890	5	130	1.380	5
20	0.957	5	140	1.344	5
21	1.016	5	150	1.310	5
22	1.064	5	160	1.275	5
23	1.102	5	180	1.214	5
24	1.133	5	200	1.161	5
25	1.158	5	250	1.056	5
26	1.181	5	300	0.966	5
27	1.200	5	350	0.890	5
28	1.217	5	400	0.826	5
29	1.234	5	450	0.771	5
30	1.263	5	500	0.724	5
31	1.321	5	600	0.647	5
32	1.401	5	700	0.585	5
33	1.524	5	800	0.536	5
34	1.642	5	900	0.495	5
35	1.709	5	1000	0.460	5
36	1.768	5	1250	0.394	5
37	1.822	5	1500	0.346	5
38	1.840	5	1750	0.309	5
39	1.852	5	2000	0.280	5

† ±0.5 eV.

‡ 90% confidence limits. This is a combination of systematic and random errors.

states formed can autoionise and will give sharp rises in the cross section. An estimate of the energies of the likely states can be made in the following way. The energies of the low-lying excited states of Ti (Corliss and Sugar 1979) are

Ti	$3p^6$	$3d^34s$	0.8–3.7 eV
		$3d^24s^2$	0 –1.5 eV
		$3d^24s4p$	2.0–5.3 eV
		$3d^24s4d$	5.1–5.9 eV.

The binding energy of a 3p electron in a Ti atom is 38 eV (Lotz 1968), so the energies of the inner-shell excited states in Ti^+ should be approximately 38 eV above

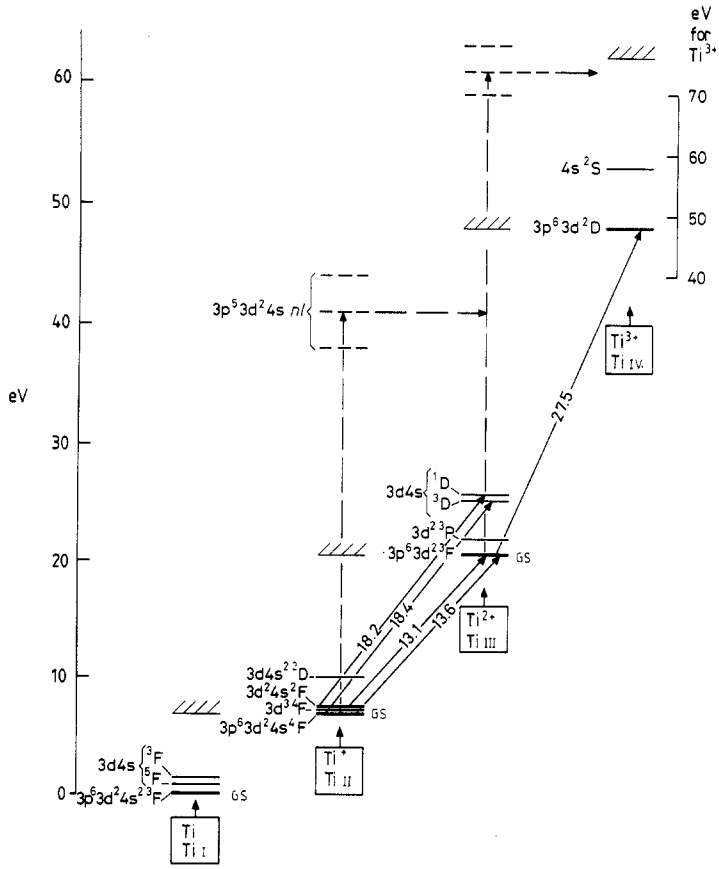

Figure 3. Simplified energy level diagram of Ti, Ti^+, Ti^{2+} and Ti^{3+} showing some of the ionising processes likely to occur (thresholds in eV). The possible excitation-autoionisation process and autoionising levels are shown as broken lines. The ground states are denoted by GS.

the states of the atom. The energies of the inner-shell excited states of Ti^+ should therefore be

Ti^+	$3p^5$	$3d^34s$	32–35 eV
		$3d^24s^2$	31–33 eV
		$3d^24s4p$	33–37 eV
		$3d^24s4d$	36–37 eV.

In the cases of ionisation of Mg^+, Ca^+, Sr^+ and Ba^+ (Peart and Dolder 1968, Martin *et al* 1968, Peart and Dolder 1975) large autoionisation contributions were observed except for Mg^+. Hansen (1975) has found that the thresholds are best fitted by theory when the $\Delta n = 0$ transition $np^6 \rightarrow np^5nd$ is responsible. This is backed up by the fact that for ionisation of Mg^+, where no $\Delta n = 0$ transitions are possible, no autoionisation cross section is found. It is likely, therefore, that the autoionisation threshold seen in Ti^+ is due to the $\Delta n = 0$ excitation:

$$Ti^+(3p^63d^24s) \rightarrow Ti^{+*}(3p^53d^34s) \rightarrow Ti^{2+}(3p^63d^2) + e$$

with a threshold energy of about 32 eV. Excitation of a 3p electron to $n = 4$ levels may contribute to the high-energy part of the autoionisation peak.

The semi-empirical formula of Lotz (1969) is in fairly good agreement with the experiment. However, this is fortuitous since the experiment indicates a large contribution from excitation-autoionisation and this process is not included in the formula. The scaled plane-wave Born cross section of McGuire (1979) is in poor agreement with the experimental data. This curve underestimates the cross section at all energies, even at high energy, where the Born approximation should be good, and below the autoionisation threshold. Again, this formula does not include an excitation-autoionisation component.

3.2. Ti^{2+}

3.2.1. Results. Most of the data for the electron impact ionisation of Ti^{2+} were taken with an ion beam energy of 4 keV, and some measurements were made with a beam energy of 6 keV as a test for possible energy-dependent errors.

The attainable Ti^{2+} beam current was small, between 2.2 and 4.4×10^{-11} A. The peak ionisation cross section for Ti^{2+} was found to be about half that of Ti^+, giving a maximum signal count rate of about 2 s^{-1} for an electron current of 250 μA. However, the stripping cross section for Ti^{2+} is also smaller than that of Ti^+ so the signal-to-background ratio remained about the same at 4:1.

It was not possible to select a beam of Ti^{3+} ions from the source so the particle detection system was calibrated using a Ti^{2+} beam. It has been shown (Peart and Harrison 1981) that the detection efficiency of electron multipliers of the type used in this experiment is dependent on ion velocity rather than energy or charge state, so that a measurement of the detection efficiency using a Ti^{2+} beam should give a good estimate of the Ti^{3+} detection efficiency for the same ion velocity. A similar method has previously been used in this laboratory (Aitken and Harrison 1971, Woodruff *et al* 1978). As a check, the detection efficiency was also measured using a 3.33 keV beam of Ar^{2+} ions and this was in satisfactory agreement with the measurement using a 4 keV beam of Ti^{2+}. Measurements of the ionisation cross section of Ti^{2+} made at the ion energies of 4 and 6 keV are in good agreement. Since separate assessments were made of the multiplier efficiency for each ion velocity, this supports the validity of the calibration. In addition, because the detection efficiency for Ti^{2+} at 6 keV was so high (0.937), i.e. approaching 100%, the efficiency for Ti^{3+} cannot be very different. The efficiency measurements are listed in table 1. The values used for determining the cross section were 0.789 at 4 keV and 0.937 at 6 keV, and the error is estimated to be ±4%.

Because of the low ion beam current the measurements of the effective beam height were less accurate than for measurements on the other ion species but the estimated error in the determination of h' did not exceed ±2%.

The data are shown in figure 4. The full circles are those taken at more than one electron current to improve the counting statistics. Also shown in the figure are the data of Mueller *et al* (1985), a curve calculated from the semi-empirical formula of Lotz (1969) and a curve calculated using the formula of Burgess and Chidichimo (1983). The low-energy region of the cross section is shown on an expanded energy scale in figure 5. The error bars shown for selected points in the figures are 90% confidence limits on the random errors. For single-electron current points these are derived from the counting statistics and for multiple current points they are derived from the least-squares-fitting procedure.

Table 3 lists values for the cross section taken from the best-fit curve drawn through the experimental points in figure 4. Also listed is the total error compounded in

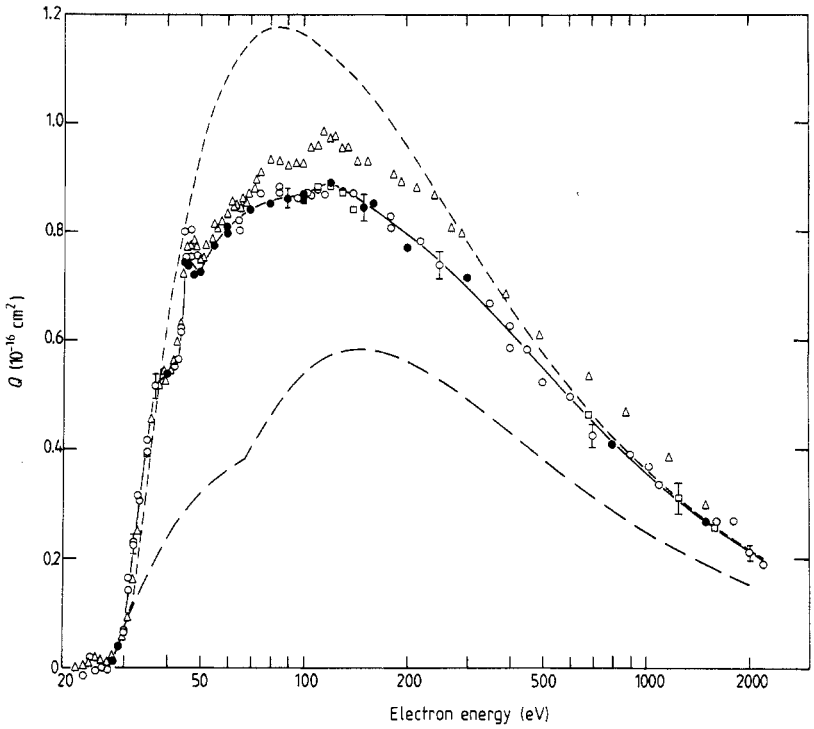

Figure 4. Electron impact ionisation cross section Q of Ti^{2+}. Present data: ○, ion energy 4 keV; □, ion energy 6 keV (full symbols indicate multiple electron current points); Δ, data of Mueller *et al* (1985); — —, semi-empirical formula of Lotz (1969); - - -, formula of Burgess and Chidichimo (1983); ——, scans and best-fit curve through experimental points.

quadrature from the random and systematic errors. Random errors are determined from the deviations of the experimental points from the fitted curve. The systematic errors are estimated to be ±4% from the multiplier calibration, ±2% from the effective beam height and ±2% from other sources.

3.2.2. Discussion. The measured cross section for ionisation of Ti^{2+} has a threshold at 27.5 eV, which corresponds to the ionisation energy of the ground state $3d^2\ ^3F$. Ions in this state can be produced from the ground state of Ti, $3d^24s^2\ ^3F$, by removal of the 4s electrons with no rearrangement of the core electrons. Other low-lying states of Ti^{2+} that can be produced directly are $3d4s\ ^3D$ and $3d4s\ ^1D$, and the states $3d^2\ ^1D$ and $3d^2\ ^3P$ can also be produced with some rearrangement of the remaining electrons. The ionisation processes possible from the directly produced states and their threshold energies are

Ti^{2+}	Ti^{3+}	
$3d^2\ ^3F$	$\rightarrow 3d\ ^2D$	27.5 eV
$3d4s\ ^3D$	$\rightarrow 3d\ ^2D$	22.8 eV
	$\rightarrow 4s\ ^2S$	32.7 eV
$3d4s\ ^1D$	$\rightarrow 3d\ ^2D$	22.3 eV
	$\rightarrow 4s\ ^2S$	32.3 eV.

The energies are calculated from the data of Corliss and Sugar (1979).

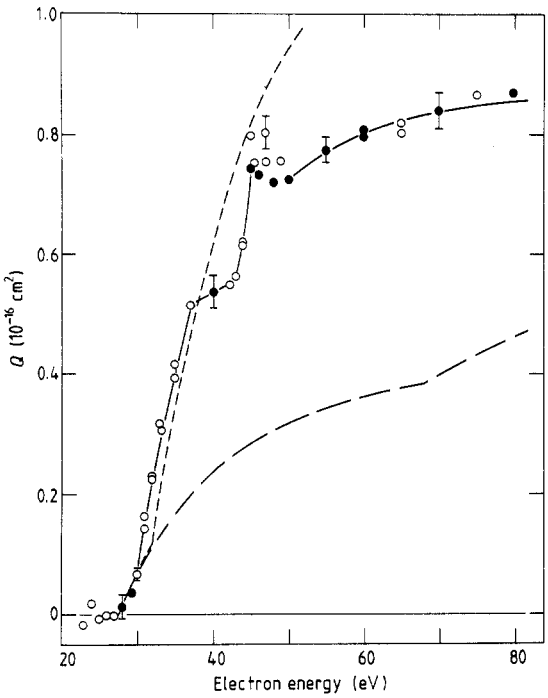

Figure 5. Ionisation cross section of Ti^{2+} shown on expanded energy scale. Symbols are the same as for figure 4.

Since no signal is observed below the ground-state threshold, we conclude that the beam does not contain a significant fraction of ions in states other than the ground state.

From the threshold to 30 eV the cross section has a gentle slope and agrees closely with that given by the formulae of Lotz and of Burgess and Chidichimo. From 30 to 37 eV there is a dramatic increase in the cross section from 0.07 to 0.52×10^{-16} cm^2, and there is a further sudden rise in the cross section at 43 eV, from where the cross section rises to a peak at 45 eV and falls to a minimum at 50 eV. These structures in the cross section are attributed to indirect ionisation processes involving excitation of a 3p electron. The energies of states with a 3p electron excited have been calculated by Griffin (1983) using relativistically modified Hartree–Fock radial wavefunctions as detailed by Griffin *et al* (1982). The energies of these states can also be estimated from an inspection of the levels in higher ionisation states, using the method described by Burgess and Chidichimo, and from the binding energies quoted by Lotz, as described for Ti^+ (§ 3.1.2). The excited states and their energies are listed in table 4. The energy ranges of all the states are broad. It is probable, as for Ti^+, that the dominant process is the $\Delta n = 0$ transition $3p^63d^2 \rightarrow 3p^53d^3$, which has its lowest energy just above 30 eV where the threshold appears in the experiment.

It was not possible in this experiment to resolve the structure between 45 and 50 eV. The energy spread (FWHM) of the electron beam has a minimum of 0.45 eV at low currents, but in order to obtain better counting statistics a higher current was used and this increased the spread to nearly 1 eV. The results suggest that the structure may have two peaks of width ≤ 0.5 eV and separated by 2 eV, but the measured peak

Table 3. Measured cross section for electron impact ionisation of Ti^{2+} taken from a smooth curve drawn through the experimental points of figure 4.

Mean electron energy† (eV)	Measured cross section Q (10^{-16} cm^2)	Total error in Q‡ (±% of Q)	Mean electron energy† (eV)	Measured cross section Q (10^{-16} cm^2)	Total error in Q‡ (±% of Q)
28	0.013	10	80	0.854	5
29	0.036	8	85	0.860	5
30	0.065	6	90	0.862	5
31	0.149	5	95	0.863	5
32	0.225	5	100	0.864	5
33	0.291	5	110	0.876	5
34	0.349	5	120	0.888	5
35	0.405	5	130	0.879	5
36	0.460	5	140	0.868	5
37	0.511	5	150	0.856	5
38	0.522	5	160	0.844	5
39	0.530	5	180	0.818	6
40	0.537	5	200	0.794	6
41	0.543	5	250	0.743	6
42	0.549	5	300	0.700	6
43	0.560	5	350	0.655	6
44	0.620	8	400	0.613	6
45	0.754	8	450	0.580	6
46	0.744	8	500	0.548	6
47	0.737	8	600	0.495	6
48	0.732	8	700	0.450	5
49	0.728	8	800	0.414	5
50	0.726	5	1000	0.357	5
55	0.773	5	1250	0.306	5
60	0.803	5	1500	0.268	5
65	0.823	5	1750	0.239	5
70	0.839	5	2000	0.216	5
75	0.848	5	2250	0.196	5

† ±0.5 eV.

‡ 90% confidence limits. This is a combination of systematic and random errors.

Table 4. Energies of inner-shell excited states of Ti^{2+}.

State	Griffin (1983) (Hartree–Fock calculations)	Burgess and Chidichimo (1983) (higher ionisation states)	Lotz (1968) (binding energies)
$3p^5 3d^3$	32–48 Average 36.7	34–49	39.5–42
$3p^5 3d^2 4s$	Average 41	54–55	39.4–42
$3p^5 3d^2 4p$	Average 46	60–64	43–44
$3p^5 3d^2 4d$	Average 51	70–72	47–48

values of $0.80\times10^{-16}\,cm^2$ were not reproducible. Structure of this type has been observed previously in the study of electron detachment from the negative ions H^- (Peart and Dolder 1973) and O^- (Peart *et al* 1979). The structures in these measurements were due to temporary capture of the incident electron with simultaneous excitation of an inner-shell electron. The resonance thus formed decays by a double autoionisation process in either one or two steps. The contribution to the ionisation cross section from this resonant-excitation-double-autoionisation (REDA) process has been calculated for Fe^{15+} by LaGattuta and Hahn (1981) and for Mg^+, Al^{2+} and Si^{3+} by Henry and Msezane (1982). This process may also contribute in the ionisation of Hf^{3+} (Bottcher *et al* 1983). If the process is responsible for the observed peak in the Ti^{2+} cross section, it would have the form

$$Ti^{2+}(3p^63d^2)+e\rightarrow Ti^+(3p^53d^2nln'l')\rightarrow Ti^{3+}(3p^63d)+2e.$$

The competition between radiative decay and double autoionisation from a resonance such as this has been considered by Trefftz (1983). The radiative decay channel is not significant for ions in low-charge states.

The semi-empirical formulae of Lotz and of Burgess and Chidichimo are both in good agreement with experiment below the first autoionisation threshold. Above this energy the Burgess and Chidichimo curve gives a reasonable approximation to the steeply rising part of the cross section but overestimates the cross section at the peak. It is again in good agreement at energies over 400 eV. The Lotz curve does not include autoionising processes and consequently underestimates the cross section at all energies above 30 eV.

The experimental results of Mueller *et al* are in good agreement with the present data. Their results show a small below-threshold signal which suggests the presence of metastable ions in the target beam. The presence of such metastable ions may explain the small discrepancy between their data and the present data above 70 eV. However, it is now clear that the structure in the cross section, which is accurately reflected in the present results, is not a consequence of the presence of metastable excited ions in the target beam.

3.3. Ar^{2+}

The cross section for electron impact ionisation of Ar^{2+} has been measured from threshold to 1250 eV. A beam of Ar^{2+} ions of about 10^{-9} A was obtained from the sputter ion source and with this beam current the signal count rate was sufficient to reduce the random errors in the measured cross section to less than the estimated systematic error. This made Ar^{2+} a good choice of species for comparison with measurements of the absolute magnitudes of the cross sections for doubly charged ions made by other groups. The cross section for Ar^{2+} has been measured in recent years by several other groups (Müller *et al* 1980, Mueller *et al* 1985, Matsumoto *et al* 1983, Danjo *et al* 1984). Such a comparison is desirable since it sets the relative magnitudes of all the measurements made at the different laboratories.

In this experiment the cross section has been measured with ion beam energies of 3.33 and 4 keV. The lower energy gave the same ion velocity as was used for the measurement on Ti^{2+} so that the particle detection efficiencies could be compared. The detection efficiency was measured with 3.33 keV Ar^{2+} ions and the value is given in table 1. A sufficient current of Ar^{3+} could not be extracted from the source to perform the calibration and so it was assumed, as for Ti^{2+}, that the efficiency did not vary with charge state.

The ion currents used were between 6×10^{-10} and 2.5×10^{-9} A, and the electron currents were between 40 and 250 μA. No problems were encountered with drifting of the detector efficiency, and so the data taken with a 4 keV ion beam were normalised to those at 3.33 keV.

The measured cross section values are plotted in figure 6 with the results of Müller *et al*, Mueller *et al* and Danjo *et al*.

The results of Müller *et al* are in good agreement with the present data, but appear to decrease more rapidly at higher energy. This is somewhat surprising since their results for singly charged ions are consistently at least 20% lower than those of other groups. However, Achenbach *et al* (1984) note that the measurements of Müller *et al* for Ar^{3+} are in good agreement with the measurements of Gregory *et al* (1983).

The results of Mueller *et al* are some 10% higher than the present data, but agree in shape, and a small cross section is apparent below the ground-state threshold. The data of Danjo *et al* appear to supersede the earlier data of Matsumoto *et al* from the same laboratory and are in good agreement with the data from other laboratories, particularly with those of Mueller *et al*. However, unlike any other data they have been taken at small energy intervals, and this, coupled with the small random errors, shows up a structure in the cross section in the region of 150 eV. The present data, which also have small random errors, do not exhibit this structure, but the energy intervals are large. In the experiment of Danjo *et al* an electron cyclotron resonance (ECR) ion source was used whereas Mueller *et al* used a dissociative source. Both

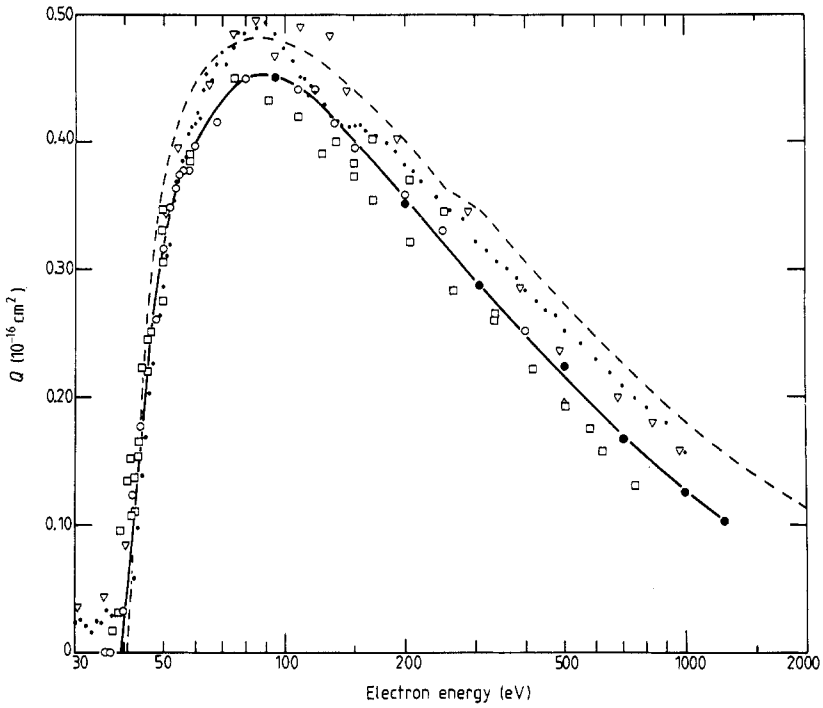

Figure 6. Electron impact ionisation cross section Q of Ar^{2+}. ○, present measurements (full symbols indicate multiple electron current points); the full curve is the best fit through the points; □, data of Müller *et al* (1980); ▽, data of Mueller *et al* (1985); ·····, data of Danjo *et al* (1984); - - -, formula of Burgess and Chidichimo (1983).

experiments show a small cross section below the ground-state threshold and a slightly enhanced maximum cross section indicating the presence of metastable excited ions in the target beam. It is tempting to suggest that the structure at 150 eV is also a manifestation of these excited ions. Further investigations are being carried out in this laboratory.

The cross section given by the Burgess and Chidichimo semi-empirical formula is in good agreement with the measured cross section over most of the energy range, but tends to overestimate the cross section at higher energies.

Table 5 lists the present measurements taken from a curve fitted to the data (the full curve in figure 5). Systematic errors are estimated to be ±1.5% from the effective beam height and 2% from other sources. These errors are compounded in quadrature with the random error determined from the deviations of the points from the fitted curve. The total error is listed in the table.

Table 5. Measured cross section for electron impact ionisation of Ar^{2+} taken from a smooth curve drawn through the experimental points of figure 6.

Mean electron energy† (eV)	Measured cross section Q (10^{-16} cm^2)	Total error in Q‡ (±% of Q)
40	0.020	20
42	0.082	10
44	0.163	6
46	0.232	5
48	0.283	5
50	0.321	5
55	0.372	5
60	0.398	5
65	0.417	5
70	0.431	5
80	0.450	5
90	0.452	5
100	0.448	5
150	0.401	5
200	0.357	5
300	0.292	5
400	0.250	5
500	0.216	5
600	0.191	5
800	0.153	5
1000	0.128	5
1250	0.102	5

† ±0.5 eV.

‡ 90% confidence limits. This is a combination of systematic and random errors.

Acknowledgments

We acknowledge the help and advice of Mr R G Montague on the crossed beam technique and also the skilled and dedicated technical assistance of Mr P R White. One of us (MJD) acknowledges the receipt of a Science and Engineering Research Council CASE Postgraduate Studentship.

References

Achenbach C, Müller A, Salzborn E and Becker R 1984 *J. Phys. B: At. Mol. Phys.* **17** 1405-25

Aitken K L and Harrison M F A 1971 *J. Phys. B: At. Mol. Phys.* **4** 1176-88

Bottcher C, Griffin D C and Pindzola M S 1983 *J. Phys. B: At. Mol. Phys.* **16** L65-70

Burgess A and Chidichimo M C 1983 *Mon. Not. R. Astron. Soc.* **203** 1269-80

Corliss C and Sugar J 1979 *J. Phys. Chem. Ref. Data* **8** 1-62

Danjo A, Matsumoto A, Ohtani S, Suzuki H, Tawara H, Wakiya K and Yoshino M 1984 *J. Phys. Soc. Japan* **53** 4091-3

Diserens M J, Harrison M F A and Smith A C H 1985 *14th Int. Conf. on the Physics of Electronic and Atomic Collisions (Palo Alto)* ed M J Coggiola, D L Huestis and R P Saxon (Amsterdam: North-Holland) Abstracts p 300

Gregory D C, Dittner P F and Crandall D H 1983 *Phys. Rev.* A **27** 724-36

Griffin D C 1983 Private communication

Griffin D C, Bottcher C and Pindzola M S 1982 *Phys. Rev.* A **25** 154-60

Hansen J E 1975 *J. Phys. B: At. Mol. Phys.* **8** 2759-70

Harting E and Read F H 1976 *Electrostatic Lenses* (Amsterdam: Elsevier)

Henry R J W and Msezane A Z 1982 *Phys. Rev.* A **26** 2545-50

Hill K J and Nelson R S 1965 *Nucl. Instrum. Methods* **38** 15-8

Klemperer O 1947 *Proc. Phys. Soc.* **59** 302-23

LaGattuta K J and Hahn Y 1981 *Phys. Rev.* A **24** 2273-6

Lotz W 1968 *J. Opt. Soc. Am.* **58** 915-21

—— 1969 *Z. Phys.* **220** 466-72

Man K F, Smith A C H and Harrison M F A 1987a *J. Phys. B: At. Mol. Phys.* **20** 4895-902

—— 1987b *J. Phys. B: At. Mol. Phys.* **20** 1351-5

—— 1987c *J. Phys. B: At. Mol. Phys.* **20** 2571-8

Martin S O, Peart B and Dolder K 1968 *J. Phys. B: At. Mol. Phys.* **1** 537-42

Matsumoto A, Ohtani S, Danjo A, Hanashiro H, Hino T, Kondo Y, Suzuki H, Tamara T, Wakiya K and Yoshino M 1983 *13th Int. Conf. on the Physics of Electronic and Atomic Collisions, Berlin* ed J Eichler *et al* (Amsterdam: North-Holland) Abstracts p 198

McGuire E J 1977 *Phys. Rev.* A **16** 73-9

Montague R G, Harrison M F A and Smith A C H 1984 *J. Phys. B: At. Mol. Phys.* **17** 3295-310

Mueller D W, Morgan T J, Dunn G H, Gregory D C and Crandall D H 1985 *Phys. Rev.* A **31** 2905-13

Müller A, Salzborn E, Frodl R, Becker R, Klein H and Winter H 1980 *J. Phys. B: At. Mol. Phys.* **13** 1877-99

Peart B and Dolder K T 1968 *J. Phys. B: At. Mol. Phys.* **1** 872-8

—— 1973 *J. Phys. B: At. Mol. Phys.* **6** 1497-502

—— 1975 *J. Phys. B: At. Mol. Phys.* **8** 56-62

Peart B, Forrest R A and Dolder K T 1979 *J. Phys. B: At. Mol. Phys.* **12** 2735-9

Peart B and Harrison M F A 1981 *J. Phys. E: Sci. Instrum.* **14** 1374

Soa E A 1959 *Jenaer Jahrbuch* **1** 115

Trefftz E 1983 *J. Phys. B: At. Mol. Phys.* **16** 1247-51

Woodruff P R, Hublet M-C, Harrison M F A and Brook E 1978 *J. Phys. B: At. Mol. Phys.* **11** L679-83